# A new plesiacerathere (Perissodactyla, Rhinocerotidae) from the late Early Miocene of northern China (#87877)



First submission

## Guidance from your Editor

Please submit by **29 Jul 2023** for the benefit of the authors (and your token reward) .

**Structure and Criteria**
Please read the 'Structure and Criteria' page for general guidance.

**Custom checks**
Make sure you include the custom checks shown below, in your review.

**Author notes**
Have you read the author notes on the guidance page?

**Raw data check**
Review the raw data.

**Image check**
Check that figures and images have not been inappropriately manipulated.

If this article is published your review will be made public. You can choose whether to sign your review. If uploading a PDF please remove any identifiable information (if you want to remain anonymous).

### Files

Download and review all files from the materials page.

4 Figure file(s)
1 Table file(s)
2 Raw data file(s)

### Custom checks

**New species checks**

- Have you checked our new species policies?
- Do you agree that it is a new species?
- Is it correctly described e.g. meets ICZN standard?

# Structure and Criteria



## Structure your review

The review form is divided into 5 sections. Please consider these when composing your review:

1. **BASIC REPORTING**
2. **EXPERIMENTAL DESIGN**
3. **VALIDITY OF THE FINDINGS**
4. General comments
5. Confidential notes to the editor

You can also annotate this PDF and upload it as part of your review

When ready submit online.

## Editorial Criteria

Use these criteria points to structure your review. The full detailed editorial criteria is on your guidance page.

### BASIC REPORTING

- Clear, unambiguous, professional English language used throughout.
- Intro & background to show context. Literature well referenced & relevant.
- Structure conforms to PeerJ standards, discipline norm, or improved for clarity.
- Figures are relevant, high quality, well labelled & described.
- Raw data supplied (see PeerJ policy).

### EXPERIMENTAL DESIGN

- Original primary research within Scope of the journal.
- Research question well defined, relevant & meaningful. It is stated how the research fills an identified knowledge gap.
- Rigorous investigation performed to a high technical & ethical standard.
- Methods described with sufficient detail & information to replicate.

### VALIDITY OF THE FINDINGS

- Impact and novelty not assessed. *Meaningful* replication encouraged where rationale & benefit to literature is clearly stated.
- All underlying data have been provided; they are robust, statistically sound, & controlled.
- Conclusions are well stated, linked to original research question & limited to supporting results.

# Standout reviewing tips



The best reviewers use these techniques

| Tip | *Example* |
| --- | --- |
| **Support criticisms with evidence from the text or from other sources** | *Smith et al (J of Methodology, 2005, V3, pp 123) have shown that the analysis you use in Lines 241-250 is not the most appropriate for this situation. Please explain why you used this method.* |
| **Give specific suggestions on how to improve the manuscript** | *Your introduction needs more detail. I suggest that you improve the description at lines 57- 86 to provide more justification for your study (specifically, you should expand upon the knowledge gap being filled).* |
| **Comment on language and grammar issues** | *The English language should be improved to ensure that an international audience can clearly understand your text. Some examples where the language could be improved include lines 23, 77, 121, 128 – the current phrasing makes comprehension difficult. I suggest you have a colleague who is proficient in English and familiar with the subject matter review your manuscript, or contact a professional editing service.* |
| **Organize by importance of the issues, and number your points** | *1. Your most important issue*<br>*2. The next most important item*<br>*3. …*<br>*4. The least important points* |
| **Please provide constructive criticism, and avoid personal opinions** | *I thank you for providing the raw data, however your supplemental files need more descriptive metadata identifiers to be useful to future readers. Although your results are compelling, the data analysis should be improved in the following ways: AA, BB, CC* |
| **Comment on strengths (as well as weaknesses) of the manuscript** | *I commend the authors for their extensive data set, compiled over many years of detailed fieldwork. In addition, the manuscript is clearly written in professional, unambiguous language. If there is a weakness, it is in the statistical analysis (as I have noted above) which should be improved upon before Acceptance.* |

# A new plesiacerathere (Perissodactyla, Rhinocerotidae) from the late Early Miocene of northern China

**Danhui Sun** [1, 2], **Tao Deng** [Corresp., 1, 2], **Shiqi Wang** [2]

[1] University of Chinese Academy of Sciences, Beijing, China

[2] Institute of Vertebrate Paleontology and Paleoanthropology, Chinese Academy of Sciences, Beijing, China

Corresponding Author: Tao Deng
Email address: dengtao@ivpp.ac.cn

Aceratheriinae is a group of rhinoceroses widely distributed in Eurasia and North America during the Miocene. As a member of Aceratheriinae, the genus *Plesiaceratherium* in Europe is widely distributed and highly diverse, but only one species of *Plesiaceratherium* (i.e. *P. gracile*) exists in China with a discontinuous distribution range. Recently, we have discovered new materials of *Plesiaceratherium* in the lower layers of the Zhang'enbao Formation exposed in Miaoerling in Tongxin County, China. The new materials are well-preserved with a series of diagnostic features: the long and generally flat skull, with a narrow distance between the sides of the parietal crests; the deep nasal notch positioned at the level of P4; the high supraorbital margin, with its anterior margin positioned at the level of the M1/M2 boundary; the short distance between the posterior edge of the nasal notch and the orbit; the ventrally closed pseudomeatus external auditory; the medium-sized upper incisor I1, with an oval abraded surface; the semi-molarized upper premolars with the protocone and hypocone joined by a lingual bridge; the strong constrictions of protocone on the upper molars; the absent buccal cingulum on upper cheek teeth. Based on the aforementioned combination of characteristics and phylogenetic analysis, we herein establish the new species as *Plesiaceratherium tongxinense* sp. nov. which survived in the late Early Miocene corresponding to the European Land Mammal Age MN 5. Phylogenetic analysis reveals that *P. tongxinense* sp. nov. is located in the basal position of the genus *Plesiaceratherium*, not only providing more detailed morphological characteristics of the plesiaceratheres but also serving as a linkage to the discontinuous distribution of the genus *Plesiaceratherium*.

# A new plesiacerathere (Perissodactyla, Rhinocerotidae) from the late Early Miocene of northern China

Danhui Sun[1,2], Tao Deng[1,2], Shiqi Wang[2]

[1] University of Chinese Academy of Sciences, Beijing, China;
[2] Key Laboratory of Vertebrate Evolution and Human Origins of Chinese Academy of Sciences, Institute of Vertebrate Paleontology and Paleoanthropology, Chinese Academy of Sciences, Beijing, China

Corresponding Author:
Tao Deng
No. 142 Xizhimenwai Street, Beijing, 100044, China
Email address: dengtao@ivpp.ac.cn

## Abstract

Aceratheriinae is a group of rhinoceroses widely distributed in Eurasia and North America during the Miocene. As a member of Aceratheriinae, the genus *Plesiaceratherium* in Europe is widely distributed and highly diverse, but only one species of *Plesiaceratherium* (i.e. *P. gracile*) exists in China with a discontinuous distribution range. Recently, we have discovered new materials of *Plesiaceratherium* in the lower layers of the Zhang'enbao Formation exposed in Miaoerling in Tongxin County, China. The new materials are well-preserved with a series of diagnostic features: the long and generally flat skull, with a narrow distance between the sides of the parietal crests; the deep nasal notch positioned at the level of P4; the high supraorbital margin, with its anterior margin positioned at the level of the M1/M2 boundary; the short distance between the posterior edge of the nasal notch and the orbit; the ventrally closed pseudomeatus external auditory; the medium-sized upper incisor I1, with an oval abraded surface; the semi-molarized upper premolars with the protocone and hypocone joined by a lingual bridge; the strong constrictions of protocone on the upper molars; the absent buccal cingulum on upper cheek teeth. Based on the aforementioned combination of characteristics and phylogenetic analysis, we herein establish the new species as *Plesiaceratherium tongxinense* sp. nov. which survived in the late Early Miocene corresponding to the European Land Mammal Age MN 5. Phylogenetic analysis reveals that *P. tongxinense* sp. nov. is located in the basal position of the genus *Plesiaceratherium*, not only providing more detailed morphological characteristics of the plesiaceratheres but also serving as a linkage to the discontinuous distribution of the genus *Plesiaceratherium*.

Keywords: *Plesiaceratherium*; osteology; phylogeny; late Early Miocene; northern China.

## Introduction

~~Add your introduction here.~~ Aceratheriinae is a group of rhinoceroses that lived in Eurasia and North America during the Miocene. As a member of Aceratheriinae, the genus *Plesiaceratherium* is well-documented throughout Eurasia (Young, 1937; Yan & Heissig, 1986; Antoine, Bulot & Ginsburg, 2000; Peter, 2002; Antoine et al., 2010). *Plesiaceratherium* is a primitive acerathere rhinoceros with elongated nasals, long but robust limb bones, and a four-toed manus (Yan & Heissig, 1986; Antoine, 2002). Young (1937) established the genus *Plesiaceratherium* based on some isolated teeth and limb bones discovered in the Early Miocene of Shanwang in Linqu, Shandong Province, China, with *P. gracile* serving as the type species. Later, Chen & Wu (1976) described some dental materials from the Miocene of Jiulongkou in Cixian, Hebei Province, China, as belonging to *P. gracile*. And then, more well-preserved materials of *Plesiaceratherium* were discovered from Shanwang, China, including many skeletons, complete skulls, and many teeth and limb bones, giving more detailed characteristics of *Plesiaceratherium* (Yan, 1983; Yan & Heissig, 1986). In addition to the discovery of *Plesiaceratherium* in eastern China, *Plesiaceratherium* also has been found in the Early Miocene of Lunbori, Baingoin County, northern Tibet, China, including a humeral material (Deng et al., 2012).

In Europe, five species have been attributed to the genus *Plesiaceratherium.* Heissig (1972) established the species *Aceratherium fahlbuschi* based on a nearly complete, uncrushed skull and numerous isolated bones, teeth and mandibular fragments (BSP 1959 Ⅱ) as a holotype discovered in the locality Sandelzhausen in Bavaria, which was later classified as *P. fahlbuschi* by Yan (1983). According to the depressed skull with mandibular, Merier (1895) established the species *Aceratherium platyodon*, afterwards referred to *P. platyodon* by Yan (1983). Antunes & Ginsburg (1983) established the species *P. lumiarense* based on right maxilla with P1-M3 as holotype from Portugal which was previously identified as *Aceratherium lumiarense* by Antunes & Ginsburg (1983). Antoine & Becker (2013) referred a species established by Répelin (1917) to *P. aquitanicum*. Becker & Tissier (2020) established a new species *P. balkanicum* based on a left premolars row as holotype from Bugojno Basin, Bosnia-Herzegovina. There was a species from the lower Miocene of Can Julia, Barcelona, Spain, referred to '*P.*' *mirallesi* by Yan (1983); however, Lu et al. (2016) considered that '*P.*' *mirallesi* should be eliminated from the genus *Plesiaceratherium*, and the initial genus name *Dromoceratherium* should be revived.

Until now, the genus *Plesiaceratherium* in Europe is widely distributed and highly diverse, but only one species of *Plesiaceratherium* (i.e. *P. gracile*) exists in China with discontinuous distribution range. Fortunately, we have recently discovered new materials of *Plesiaceratherium* in Tongxin County, Ningxia Hui Autonomous Region, China. The Tongxin region, which was impacted by tectonic activity, contains an abundance and continuous deposit of Cenozoic sediments (Wang et al., 2011, 2016). Our new plesiacerathere materials reported here were found in the lower layers of the Zhang'enbao Formation exposed in Miaoerling, which dates to the European Land Mammal Age MN5 (Wang et al., 2016). The studied materials allow describing a new species of plesiacerathere, *Plesiaceratherium tongxinense* sp. nov., not only providing more

detailed multiple characters of *Plesiaceratherium*, but also serving as a linkage to the discontinuous distribution of the genus.

## Materials & Methods

The fossils for this study are an adult skull and mandibular discovered in Tongxin, Ningxia Hui Autonomous Region, China, stored in the collection of the Institute of Vertebrate Paleontology and Paleoanthropology (IVPP), Chinese Academy of Sciences, Beijing, China. The fossils are described and identified through anatomical descriptions, comparative anatomy as well as biometrical measurements. Rhinocerotid terminology and taxonomy follow Heissig (1972, 1999), Guérin (1980), and Antoine (2002). Anatomical features described follow basically the same sequence as in Antoine (2002), and Antoine *et al.* (2010). The specimens were measured in accordance with the procedures described in Guérin (1980).

The phylogenetic analysis in this paper is performed using a modified data matrix from Antoine (2002, 2003) in order to assess the phylogenetic position of the new specimen (Appendix). The matrix analyzed in the present study contains 282 morphological characters including 52 cranial characters, 10 mandibular characters, 120 dental characters, and 100 postcranial characters. The phylogenetic analysis was performed using a traditional search under TNT (Version 1.1) (Goloboff, Farris & Nixon, 2008), with all multistate characters treated as additive, except for the characters 72, 94, 102, 140, and 187 (non-additive). The current matrix consists of 30 taxa coded at the species level.

**Institutional abbreviations**

**I/i**, upper/lower incisor, **M/m**, upper/lower molar, **and P/p**, upper/lower premolar. **L**, length, and **W**, width. **BSP**, Bayerische Staatssammlung für Paläontologie und Geologie, Münich, Germany; **MNHN**, Muséum National d'Histoire Naturelle, Paris, France; and **IVPP**, Institute of Vertebrate Paleontology and Paleoanthropology, Chinese Academy of Sciences, Beijing, China.

## Results

**Systematic paleontology**

Order **Perissodactyla** Owen, 1848

Family **Rhinocerotidae** Gray, 1821

Subfamily **Aceratheriinae** Dollo, 1885

Tribe **Aceratheriini** Dollo, 1885

Genus ***Plesiaceratherium*** Young, 1937

**Type species.** *Plesiaceratherium gracile* Young, 1937

**Other species.** *P. platyodon* (Mermier, 1895), *P. aquitanicum* (Répelin, 1917), *P. fahlbuschi* (Heissig, 1972), *P. lumiarense* (Antunes & Ginsburg, 1983), *P. naricum* (Pilgrim, 1910), *P. balkanicum* Becker & Tissier, 2020, *P. tongxinense* sp. nov.

**Revised Diagnosis.** Medium to large-sized primitive aceratheriine; limb bones more slender than in other Miocene aceratheriine genera; the nasal bones are elongated and straight, with a deep nasal notch at the level of P4; I1 is medium-sized, i2 is large and slightly curved; the upper cheek

teeth have low crowns; the upper premolars are semi-molarized; the lower premolars are narrow and long, with relatively shallow ectoflexid (Yan & Heissig, 1986; Lu et al., 2016).

**Distribution.** Early Miocene (MN 1-5), Eurasia.

***Plesiaceratherium tongxinense*** sp. nov.

(Figs 1-4; Tables 1-3)

**Holotype.** IVPP V23959, a well-preserved and complete skull and mandible (Fig. 1-3) representing a full adult individual, which are preserved at the Institute of Vertebrate Paleontology and Paleoanthropology, Chinese Academy of Sciences, Beijing, China.

**Derivation of name.** The specific name, tongxinense, refers to the geographical location of the discovery.

**Type locality and horizon.** Miaoerling in Shishi Township, Tongxin County, Ningxia Hui Autonomous Region, China; late Early Miocene.

**Diagnosis.** The skull is long and relatively flat, with a distance between the sides of the parietal crests; the nasal notch is deep and located at the level of P4; the supraorbital margin is high and its anterior margin is located at the level of the M1/M2 boundary; the distance between the posterior edge of the nasal notch and the orbit is short; the pseudomeatus external auditory is closed ventrally; the upper incisor I1 is developed and specialized, medium in size, with an oval abraded surface; the upper cheek teeth are low crowned; the upper premolars are semi-molarized with the protocone and hypocone connected with each other by a lingual bridge; the protocone on the upper molars has developed anterior and posterior constrictions; the buccal cingulum is absent on upper cheek teeth.

**Description**

**Skull.** The skull of IVPP V 23559 is complete and well-preserved with the upper cheek teeth moderately worn. The skull was slightly deformed by lateral compression, with the frontal and posterior part of the nasal bones collapsed downward at the middle suture, the basioccipital and basal pterygoid parts narrowed, and the palatal bones deeply sunken while keeping the tooth rows close together.

In the lateral view, the dorsal skull profile is flat and long. The occipital part is slightly raised, and its profile is almost vertical. The occipital condyle is low and small. The posttympanic process is short and fused with the paraoccipital process, and anteriorly touches the postglenoid process. The pseudomeatus external auditory is closed ventrally, and its upper edge is short located in the lower half of the occipital crest. The area between the temporal and occipital crests is depressed. The zygomatic arch is fairly thin (particularly the middle part), the anterior end of which is located at the level of M1 and close to the cheek teeth row, and the posterior end of the dorsal edge has a short process. The temporal condyle that is articulated with the mandible is protruding from the ventral edge of the zygomatic arch. The postglenoid process is laterally flattened. The position of the dorsal margin of the orbit is high, and the anterior margin of the orbit is located at the level of the M1/M2 boundary. The supraorbital edge of the frontal bone has a coarse area but lacks any process or tubercle. The posterior orbital border is formed by the zygomatic bone, and presents a coarse area, without any tubercles. The nasal bone is thin and flat

without lateral apophyses on both sides. The nasal notch has a U-shaped outline, and its posterior edge is at the level of the middle part of P4. The distance between the posterior edge of the nasal notch and the orbit is short, about 67 mm. The infraorbital foramen is located dorsally to the level of P4 and posteriorly to the nasal notch. The premaxillary bones are fairly well-saved with deeply abraded I1s.

In the dorsal view, the parietal crests are not fused to a sagittal crest, and the smallest width between parietal crests is located anterior to the nuchal crest, about 35 mm. The frontals are constricted at the middle of the temporal fossa. The ratio of zygomatic width to frontal width is more than 1.5. The postorbital process is present. The widest position of the dorsal surface is located between the supraorbital processes, about 139 mm. The nasal bone becomes narrow gradually before the orbits (i.e., the nasal base does not have a constriction). The nasal bone is narrow, flat, and long with a nasal suture.

In the ventral view, the skull is long with a length (from premaxilla to occipital condyle) of 584mm. The ventral and occipital surfaces of the occipital condyle are rounded, without a median ridge. The hypoglossal foramen is laterally positioned, at the basement of the paraoccipital process. The posttympanic process is and fused with the paraoccipital process, and anteriorly touches the postglenoid process. The alar foramen is opened on the lateral wall of the posterior nares, anteroposteriorally at the level of the temporal condyle. The tympanic bulla has been crushed, exposing the inner bones. The temporal condyle is high, and its transverse axis is straight. The posterior margins of pterygoid are nearly vertical. The anterior edge of the posterior nares is V-shaped in outline, at the level of M3. The posterior edge of the lateral wall of the posterior nares with a steep part is continuous, extending to the foramen lacerum anterius that is at the back of the level of the temporal condyle. The medial and lateral edges of the cheek tooth row are nearly straight. The slender and straight premaxillary bones are two separated and faintly paralleled plates with a length of 66.7 mm. I1 is deeply abraded and oval-shaped.

In the posterior view, the occipital face is bell-shaped in outline, and the upper part is narrower than the lower part. The occipital crest is rounded above and gradually inclined laterally. The nuchal tuberosity is developed. The foramen magnum is small, rounded in shape, and its width is 38 mm. The occipital condyles are relatively small, and its lateral margin has a short and steep upper part, and a long and curved lower part. The width between exterior edges of occipital condyles is 97 mm.

**Upper teeth.** The upper teeth are moderately worn. The upper cheek tooth row is almost in a straight line posteriorly positioned relative to the orbit. The ratio of the length of the upper premolars (P3-4) to the molars (M1-3) is low, about 45%. On the upper cheek teeth, the buccal wall undulates; the expansion of the lingual cusps is developed; the protocone is constricted anteroposteriorly; and the enamel foldings are absent. On the premolars, the lingual cingulum is present and continuous; the medisinus is closed; there is a lingual bridge between the protocone and hypocone; the protocone is constricted, and its lingual margin is curved; and the postfossette is narrow and closed. On the molars, the antecrochet is developed; the crochet is developed but

the crista is absent; the buccal cingulum is absent, but the lingual cingulum is present; and the protocone and hypocone are strongly constricted.
I1 is oval-shaped in the middle size with a longitudinal length of 26.5 mm in the cross-section.
DP1 is not saved.
P2 is nearly quadrangular in occlusal view with a relatively flat buccal wall. The parastyle fold and the paracone rib are weak. The protocone and hypocone connect with each other by a lingual bridge. The hypocone is marginally larger than the protocone. The hypocone is at the same level as that of the metacone. The protoloph is as buccally narrow as the metaloph, and joins with the ectoloph. The crochet and crista are connected forming a medifossette. Both the medisinus and the postfossette are closed. The anterior and the posterior cingula are developed. The lingual cingulum is V-shaped at the entrance of the medisinus. The buccal cingulum is absent.
P3 has a weak parastyle fold and paracone rib with a shallowly undulating buccal wall. The hypocone has an anterior constriction. The protocone and hypocone connect with each other by a lingual bridge. The protocone is slightly larger than the hypocone. The crochet and crista are developed. The medisinus is narrow and closed. The postfossette is small in a round shape. The lingual cingulum is developed and continuous and the buccal cingulum is absent.
P4 is similar to P3, but much larger. The hypocone is expanded, with slight anterior constriction. The protocone is slightly smaller than the hypocone. The lingual margin of the protocone is curved. The protoloph is longer than the metaloph. The lingual cingulum is developed and continuous. The buccal cingulum is absent.
M1 has a projecting parastyle with an undulating buccal wall. The strongly constricted protocone has a flat lingual margin, and the hypocone has a strong anterior constriction. The antecrochet is strong and elongates to the entrance of the medisinus. The medisinus leans to the rear which is narrow. The postfossette is round in shape and closed. The anterior cingulum is developed, and the lingual cingulum is reduced, forming a pillar around the entrance of the medisinus. The buccal cingulum is absent.
M2 has a long parastyle and a developed parastyle fold, and a paracone rib with an undulating buccal wall. The protocone has developed anterior and posterior constrictions. The hypocone has a strong anterior constriction. The crochet is well-developed. The antecrochet is strongly developed, and the stout end extends to the entrance of the medisinus. The antecrochet and hypocone are separated. M2 has an open medisinus, an oval-shaped and closed postfossette. M2 has well-developed anterior and cingulum, and the lingual cingulum is reduced, forming a pillar around the entrance of the medisinus. The buccal cingulum is absent.
M3 has a quadrangular outline in occlusal view. It has a short and sharp parastyle, a wide protoloph, and an ectometaloph. The protoloph is transverse on the antero-lingual side. The crochet is well-developed but does not form a medifossette. The protocone has anterior and posterior constrictions. The anterior cingulum is well developed and continuous, and the posterior and lingual cingula are reduced, forming a pillar respectively.
**Mandible:** The mandible of IVPP V 23559 is well-preserved with the lower cheek teeth moderately worn. The mandible was slightly deformed by extrusion from the right to left

direction. The right i2 is broken, and the left p2 is lost. The horizontal ramus is long and raised. The lower margin is fairly concave under the cheek teeth, with an upturned mandibular symphysis. The length of the mandibular symphysis along median plane is long, about 153 mm. The posterior border of the mandibular symphysis is situated at the level of the p3. The oval mental foramen is small and located in the lower half of the horizontal ramus at the level before p2. The ascending ramus is relatively high with a height of 278 mm at the coronoid process, and 238 mm at the condyloid process. The mandibular condyle is transversely extended with a width of 87 mm, corresponding to the length of the glenoid fossa of the skull. The medial end of the condyloid process is curved posteriorly. The lateral half of the condyle is slightly inclined anteriorly. The mandibular notch between the coronoid and condyloid processes is narrow and deep. The lower part of the coronoid process is wide antero-posteriorly, and the upper part above the condyloid process tapers gradually as it curves posteriorly, with a flat anterior margin and rounded posterior margin. The posterior margin of the ascending ramus is slightly posteriorly inclined. The mandibular angle is rounded forming an obtuse angle. On the lateral surface of the ascending ramus, the masseter fossa is very deep under the coronoid process. The medial surface of the ascending ramus is depressed. The mandibular foramen is very large and situated anteriorly, with its bottom above the alveolar level. The groove behind the mandibular foramen is deep and wide, extending upward.

**Lower teeth:** The lower teeth are moderately worn. The row of the lower cheek teeth is aligned with the longitudinal axis of the horizontal ramus.

The i2 is medium-sized, dagger-shaped, and extending obliquely forward and upward almost parallel, with a root thicker than the crown. Its transverse section is a round triangle with an interior sharp angle, and the cross section of the root is oval.

The p2 is small in a triangular shape. It has a short and wide protolophid and a shallow ectoflexid. The trigonid basin is small and open, and the talonid basin is rounded and nearly disappeared. The buccal cingulum is developed under the hypolophid but absent under the protolophid.

The p3 is trapezoid in the occlusal view, with a slightly shorter anterior margin than the posterior one. The postero-buccal corner of the protoconid is rounded. The ectoflexid is shallow. The metalophid is robust, much wider than the entolophid. The trigonid basin is small and shallowly V-shaped, and the talonid basin is deeply V-shaped. The lingual cingulum is developed, and the buccal cingulum is developed under the hypolophid but absent under the protolophid.

The p4 is similar to p3 in morphology, but bigger in size: The occlusal surface is nearly rectangular. The postero-buccal corner of the protoconid is more angular than that of p3. The ectoflexid is wider and deeper than that of p3. The trigonid basin is nearly disappeared, and the talonid basin is deeply V-shaped.

The m1 is deeply worn. The occlusal surface is nearly rectangular. The postero-buccal corner of the protoconid is nearly right-angled. The ectoflexid is wide and shallow. The trigonid basin is nearly disappeared, and the talonid basin is deeply V-shaped. The lingual cingulum is reduced, and the buccal cingulum is absent.

The m2 has a rectangular occlusal surface. The postero-buccal corner of the protoconid is right-angled. The ectoflexid is shallowly V-shaped. The metalophid is robust and wider than the entolophid. The trigonid basin is U-shaped and the talonid basin is deeply V-shaped. Both the protolophid and hypolophid are slightly lingually oblique. The buccal cingulum is absent and the lingual cingulum is reduced.

The m3 has a trapezoid occlusal surface, with slightly shorter anterior margin than the posterior one. The postero-buccal corner of the protoconid is right-angled. The ectoflexid is wide and shallow. The metalophid is robust and wider than the entolophid. The trigonid basin is nearly disappeared, and the talonid basin is deeply V-shaped. Both the protolophid and hypolophid are slightly lingually oblique. The buccal cingulum is absent and the lingual cingulum is reduced.

## Comparison and Discussion

The well-preserved new materials (IVPP V23959) from Tongxin, Ningxia have typical features easily recognizable as typical of aceratheriine, including a flat and long nasal bone with a retracted nasal notch; the posttympanic process fused with the paraoccipital process; the upturned mandibular symphysis with large and straight i2s; the constricted lingual cusps on the upper cheek teeth.

Compared with the aceratheriines, the Tongxin specimen differs in the morphology of the skull and mandibular, as well as the degree of specialization of the incisors and cheek teeth. The Tongxin specimen differs from *Mesaceratherium* living in Eurasia from the upper Oligocene to lower Miocene by the relatively smaller I1s, and more complex occlusal patterns of the upper cheek teeth (Heissig, 1969; Blanchon et al., 2018). The Tongxin specimen also differs from *Alicornops* by the relatively smaller I1s, shorter distance from the nasal notch to the orbit, relatively low nuchal crest above the parietal and frontal surfaces, the reduction of buccal and lingual cingulum of lower molars, and the presence of a medifossette on upper premolars and a longer crochet on upper molars (Cerdeño & Sanchez, 2000; Deng, 2004; Heissig, 2012). The Tongxin specimen with developed I1s is clearly different from the derived Eurasian aceratheriines, such as *Hoploaceratherium*, *Chilotherium*, *Acerorhinus*, *Subchilotherium*, and *Shansirhinus* (Borissiak, 1915; Ringström, 1924; Colbert, 1935; Deng, 2005; Heissig, 2012) However, the Tongxin specimen shares diagnostic characters with the genus *Plesiaceratherium*, such as the narrow and slightly raised nuchal crest; the posttympanic process anteriorly touches the postglenoid process; the ventrally closed pseudomeatus external auditory; the nasal notch retracted to the level of P4; the upturned mandibular symphysis with large and straight i2s; the medium-sized I1s; the constricted lingual cusps on the upper cheek teeth; the narrow and long lower premolars with relatively shallow ectoflexid. Therefore, based on the combination of characters, we refer the Tongxin specimen to the genus *Plesiaceratherium* (Young, 1937; Yan, 1983; Yan & Heissig, 1986).

Compared with *P. gracile* (Young, 1937; Lu et al., 2016), the Tongxin specimen differs by the relatively wide parietal crests, but those of *P. gracile* are fused to form a single sagittal crest. The anterior margin of the orbit of the Tongxin specimen is retracted at the level of the M1/M2

boundary, while that of *P. gracile* is located at the level of M1. The constrictions of the protocone and hypocone on the upper molars of the Tongxin specimen are stronger than those of *P. gracile*. The antecrochet and crochet on the upper molars of the Tongxin specimen are developed and stout, whereas *P. gracile* has slightly developed antecrochet and slender crochet on the upper molars. The crista on the upper molars of the Tongxin specimen is absent, but that of *P. gracile* is present. The cheek teeth of the Tongxin specimen are covered by cement on the buccal walls different from that of *P. gracile* without cement.

Different from *P. fahlbuschi* (Heissig, 1972), the Tongxin specimen is larger in size than *P. fahlbuschi*. The distance between the posterior edge of the nasal notch and the orbit the Tongxin specimen is longer than that of *P. fahlbuschi*, which respectively are about 67 mm and 43-35 mm. The parietal crests of the Tongxin specimen are relatively wide, but those of *P. fahlbuschi* are fused to form a single sagittal crest. The anterior margin of the orbit of the Tongxin specimen is retracted at the level of the M1/M2 boundary, and that of *P. fahlbuschi* is located at the level of middle part of M1. The Tongxin specimen has semi-molarized upper premolars with the protocone and hypocone connected with each other by a lingual bridge, while *P. fahlbuschi* has molarized upper premolars with the protocone and hypocone separated.

Compared with *P. platyodon*, the Tongxin specimen is larger in size than *P. platyodon*. The distance between the posterior edge of the nasal notch and the orbit the Tongxin specimen is about 67 mm longer than that of *P. platyodon* about 58mm. The anterior margin of the orbit of the Tongxin specimen is retracted at the level of the M1/M2 boundary, and that of *P. platyodon* is located at the level of middle part of M1. The crochet on the upper molars of the Tongxin specimen is developed and stout, whereas that of *P. platyodon* is weak or absent. The M3 of the Tongxin specimen has a quadrangular outline in occlusal view, while that of *P. platyodon* has a triangular outline.

In addition, there are other species within the genus *Plesiaceratherium* and the preserved materials are scarce. Compared with *P. lumiarense*, the Tongxin specimen has semi-molarized upper premolars with the protocone and hypocone connected with each other by a lingual bridge, while *P. lumiarense* has upper premolars with the protocone and hypocone mostly separated. The Tongxin specimen differs from *P. aquitanicum* by the features as follows. The protoloph of the Tongxin specimen joins with the ectoloph on P2 but that of *P. aquitanicum* is separated from the ectoloph. The crista on the upper molars of the Tongxin specimen is absent, but that of *P. aquitanicum* is present. The M3 of the Tongxin specimen has a quadrangular outline in occlusal view, while that of *P. aquitanicum* has a triangular outline. Different from *P. balkanicum*, the Tongxin specimen has semi-molarized upper premolars with the protocone and hypocone connected with each other by a lingual bridge, while *P. balkanicum* has molarized upper premolars with the protocone and hypocone separated. The protoloph of the Tongxin specimen joins with the ectoloph on P2 but that of *P. balkanicum* is separated from the ectoloph. Therefore, the Tongxin specimen is obviously distinguished from all known species of the genus *Plesiaceratherium* by a unique combination of characters: the skull is long and relatively flat with separated parietal crests; the supraorbital margin is high and its anterior margin is located at

the level of the M1/M2 boundary; the upper incisor I1 is developed and specialized, medium in size, with an oval abraded surface; the upper premolars are semi-molarized with the protocone and hypocone connected with each other by a lingual bridge; the protocone on the upper molars has developed anterior and posterior constrictions; the buccal cingulum is absent on upper cheek teeth; the M3 has a quadrangular outline in occlusal view. Based on those, we attribute the Tongxin specimen to a new species, *P. tongxinense* sp. nov.

Although retaining some primitive characters, *Plesiaceratherium* is already a rather specialized genus, such as the complex occlusal surface of the upper cheek teeth, the rather deep nasal incision, and the ventrally closed pseudomeatus external auditory, representing an earlier specialized taxon within Aceratheriinae (Yan & Heissig, 1986). As far as the dentition is concerned, *Aceratherium* and *Plesiaceratherium* are almost indistinguishable, and the skull characters are also fairly similar (Yan, 1983). Therefore, the study of postcranials will be necessary to further understand the relationship between *Aceratherium* and *Plesiaceratherium* and to establish the phylogenetic position of *Plesiaceratherium*.

The genus *Plesiaceratherium* is widely distributed in Eurasia with various occurrences in China, South Asia, and Europe (Young, 1937; Yan & Heissig, 1986; Antoine, Bulot & Ginsburg, 2000; Peter, 2002; Antoine et al., 2010). The earliest representative of this genus is *P. naricum*, from the earliest Miocene of Pakistan (MN1-MN2) (Antoine et al., 2010, 2013; Antoine & Becker, 2013). In Europe, *Plesiaceratherium* was previously discovered in six localities, Sandelzhausen and Voggersberg in Germany, Pont du Manne as well as Estrepouy in France, Charneca de Lumiar in Portugal, and Can Julia in Spain (Heissig 1999; Antoine & Becker 2013). In China, *Plesiaceratherium* was found in three localities, namely, Shanwang in Linqu, Shandong Province (Young 1937; Yan & Heissig 1986), Jiulongkou in Cixian, Hebei Province (Chen & Wu, 1976), and Lunbori in Baingoin, northern Tibet (Deng et al., 2012). According to the published data, the age of the Shanwang Fauna was about 18 Ma (Deng, Wang & Yue, 2003; Deng et al., 2012), and the fossil locality of the Jiulongkou Fauna should be the latest Shanwangian Age at about 16 Ma (Deng et al., 2012). In addition, the upper part of the Dingqing Formation at the Lunbori locality bearing *Plesiaceratherium* fossil is characteristic of the Early Miocene (Deng et al., 2012). Moreover, the localities yielding the more progressed *Plesiaceratherium* in Europe belong to MN 4 or 5 of the mammalian ages at 18-15 Ma (Steininger, 1999; Deng et al., 2012). Thus, the localities in *Plesiaceratherium*'s distribution in Eurasia are very close in age, i.e. the late Early Miocene.

The new fossil materials of *Plesiaceratherium* reported here were discovered in the lower part of the Zhang'enbao Formation exposed in Miaoerling, corresponding to the European Land Mammal Age MN5 (Wang et al., 2016). Besides, according to Wang (2021), the magnetostratigraphic analyses currently implied an age MN5 (late Early Miocene) for the locality Miaoerling, which is consistent with the observed rhinoceroses association. Therefore, *P. tongxinense* sp. nov. survived in the late Early Miocene.

## Phylogenetic analysis

In order to explore the phylogeny of the Tongxin specimen, we performed a phylogenetic analysis of the Rhinocerotidae (based on the data matrix of Antoine (2002, 2003), with the addition of *Plesiaceratherium tongxinense* sp. nov., *P. fahlbuschi*, *P. gracile*, *P. lumiarense*, and *P. platyodon*, resulting in four equally most parsimonious trees. The tree length is 989 steps, with a consistency index of 0.371 and a retention index of 0.602.

The members of Teleoceratina are located in a stable monophyletic clade (Node A) (Fig. 4). They share twenty-four equivocal synapomorphies including the concave dorsal profile of skull ($15^{0-1}$), the distant processus posttympanicus and processus paraoccipitalis ($46^{0-1}$), the subtriangular foramen magnum ($49^{0-1}$), the constricted metaconid on lower cheekteeth ($144^{0-1}$), the usually absent d1/p1 (in adults) ($151^{1-2}$), the usually open posterior valley on d2 ($180^{0-1}$), the usually fused proximal ulna-facets of radius ($199^{0-2}$), the weak gutter for the m. extensor carpi of radius ($202^{0-1}$), the closed angle between diaphysis and olecranon of ulna ($205^{0-1}$), the present anterior tubercle on the distal end of ulna ($206^{0-1}$), the short posterior tuberosity of magnum ($220^{1-0}$), the straight magnum-facet of McII ($224^{0-1}$), the invisible magnum-facet in anterior view of McIII ($229^{0-1}$), the vestigial McV ($231^{0-1}$), the salient insertion of the m. extensor carpalis of metacarpals ($232^{0-1}$), the straight proximal border of the patellar trochlea of femur ($241^{0-1}$), the usually present medio-distal gutter (tendon m. tibialis posterior) of tibia ($243^{0-1}$), the ratio of transverse diameter/height of astragalus ≥1.2 ($252^{1-2}$), the absent posterior stop on the cuboid-facet of astragalus ($257^{0-1}$), the nearly flat calcaneus-facet of astragalus ($262^{0-1}$), the usually present fibula-facet of calcaneus ($264^{1-2}$), the present cuboid-facet of MtIII ($275^{0-1}$), the robust limbs ($279^{0-1}$), the present postero-distal tubercle on the diaphysis of central metapodials ($281^{0-1}$).

The clade (Node B) includes the plesiaceratheres (Fig. 4) supporting by twelve equivocal synapomorphies including the very long nasal bones ($26^{0-2}$), the absent i1 ($76^{0-1}$), the always simple crochet on P2-4 ($85^{1-0}$), the postfossette on P2-4 with posterior wall ($89^{0-2}$), the protoloph on P2 joined to the ectoloph ($99^{1-0}$), the usually absent constriction of the protocone on P3-4 ($101^{0-1}$), the always present crista on P3 ($105^{1.2-3}$), the absent metacone fold on M1-2 ($119^{0-1}$), the low and reduced posterior cingulum on M1-2 ($124^{0-1}$), the always present constriction of the protocone on M3 ($135^{0-2}$), the present vertical external rugosities on p2-3 ($139^{0-1}$), and the reduced labial cingulum on lower premolars ($150^{0-1}$). The new species *Plesiaceratherium tongxinense* sp. nov. established here is located in the basal position of the genus *Plesiaceratherium* supporting by nineteen equivocal synapomorphies including the close frontoparietal crests ($35^{0-1}$), the high articular tubercle of squamosal ($39^{0-1}$), the dihedron processus postglenoidalis of squamosal ($42^{1-2}$), the absent sagittal crest on the basilar process ($44^{1-0}$), the inclined backward ramus ($60^{0.1-2}$), the foramen mandibulare above the teeth neck ($62^{0-1}$), the radio of compared length of the premolars/molars rows between 42% to 50% ($63^{0-1}$), the present cement on cheekteeth ($65^{0-1}$), the divergent orientation of i2 ($80^{0-1}$), the present metaloph constriction on P2-4 ($86^{0-1}$), the always present antecrochet on P2-3 ($90^{0-3}$), the protocone on P2 less strong than the hypocone ($97^{0-1}$), the always present medifossette on P3-4 ($100^{0-3}$), the always present constriction of the protocone on P3-4 ($101^{1-3}$), the the lingual bridge existing between protocone and hypocone on P3-4 ($102^{2-1}$), the strong constriction of the

protocone on M1-2 ($116^{0-1}$), the continuous metaloph on M2 ($129^{1-0}$), the external groove developed until the neck on lower cheekteeth ($141^{0-1}$), the rounded trigonid on lower cheekteeth ($142^{0-1}$). The scarcity of fossil material of *P. tongxinense* sp. nov. suggests that it may be at an early stage, while the later flourishing of *P. gracile* and the diversity of European *Plesiaceratherium* indicate that the genus has reached an adaptive radiation stage.

The clade (Node C) containing elasmotheres (Fig. 4) is supported by thirty-two equivocal synapomorphies including the radio of compared length of the premolars/molars rows between 42% to 50% ($63^{0-1}$), the always simple crochet on P2-4 ($85^{1-0}$), the always absent lingual cingulum on P2-4 ($87^{0-3}$), the wide postfossette on P2-4 ($89^{0-1}$), the lingual wall existing between protocone and hypocone on P2 ($94^{1-3}$), the transverse metaloph on P2 ($95^{0-1}$), the lingual wall existing between protocone and hypocone on P3-4 ($102^{2-3}$), the usually present lingual cingulum on upper molars ($114^{0-1}$), the always present constriction of the protocone on M3 ($135^{0-2}$), the usually absent on lingual cingulum lower premolars ($147^{0-2}$), the absent labial cingulum on lower premolars ($149^{0-1}$), the usually present lingual cingulum on lower molars ($157^{0-1}$), the deep latero-distal gutter (tendon peronaeus muscles) of fibula ($250^{0-1}$), the median position of the latero-distal gutter of fibula ($251^{0-1}$), the pad-shaped and continuous postero-proximal tuberosity of MtIV ($277^{0-1}$). *Diceratherium armatum* and *Menoceras arikarense* are the sister-groups of Elasmotheriina (i.e. elasmotheriines sensu stricto) which is consistent with the results of Antoine's (2003) phylogenetic analysis.

## Conclusions

The particularly complete skull and mandible from (IVPP V23959) from Tongxin, Ningxia described here does not quite match any known aceratheres. Although the skull and mandible conform to the generic characters of *Plesiaceratherium*, it also differs from the known species of this genus. The Tongxin specimen is well-preserved with a series of identification features. The skull is long and generally flat, with a distance between the sides of the parietal crests; the nasal notch is deep positioned at the level of P4; the supraorbital margin is high, with its anterior margin positioned at the level of the M1/M2 boundary; there is a short distance between the posterior edge of the nasal notch and the orbit; the pseudomeatus external auditory is closed ventrally. The upper incisor I1 is developed and specialized, medium in size, with an oval abraded surface; the upper cheek teeth have low crowns; the upper premolars are semi-molarized with the protocone and hypocone joined by a lingual bridge; the protocone on the upper molars has developed anterior and posterior constrictions; the buccal cingulum is absent on upper cheek teeth. As a result, based on the aforementioned combination of characteristics and phylogenetic analysis, we herein establish the new species as *Plesiaceratherium tongxinense* sp. nov. surviving in the late Early Miocene corresponding to the European Land Mammal Age MN 5. Phylogenetic analysis reveals that *P. tongxinense* sp. nov. is located in the basal position of the genus *Plesiaceratherium* supporting by nineteen equivocal synapomorphies including the close frontoparietal crests, the high articular tubercle of squamosal, the dihedron processus postglenoidalis of squamosal, the absent sagittal crest on the basilar process, the inclined

backward ramus, the foramen mandibulare above the teeth neck, the radio of compared length of the premolars/molars rows between 42% to 50%, the present cement on cheekteeth, the divergent orientation of i2, the present metaloph constriction on P2-4, the always present antecrochet on P2-3, the protocone on P2 less strong than the hypocone, the always present medifossette on P3-4, the always present constriction of the protocone on P3-4, the the lingual bridge existing between protocone and hypocone on P3-4, the strong constriction of the protocone on M1-2, the continuous metaloph on M2, the external groove developed until the neck on lower cheekteeth, the rounded trigonid on lower cheekteeth. The discovery of new specimen not only improves the morphological characteristics but also increases the diversity of the plesiaceratheres, serving as a linkage to the discontinuous distribution of the genus *Plesiaceratherium*.

## Acknowledgements

We thank Prof. Zhanxiang Qiu for his constructive suggestions and comments. We thank Wei Gao for his photographs, Xiaocong Guo for her illustrations.

## References

Antoine P-O. 2002. *Phylogénie et évolution des Elasmotheriina (Mammalia, Rhinocerotidae)*. Mémoires du Muséum National d'Histoire Naturelle 188.

Antoine P-O. 2003. Middle Miocene elasmotheriine Rhinocerotidae from China and Mongolia: taxonomic revision and phylogenetic relationships. *Zoologica Scripta* 32:95–118. DOI: 10.1046/j.1463-6409.2003.00106.x.

Antoine P-O, Becker D. 2013. A brief review of Agenian rhinocerotids in Western Europe. *Swiss Journal of Geosciences* 106:135–146. DOI: 10.1007/s00015-013-0126-8.

Antoine P-O, Bulot C, Ginsburg L. 2000. Une faune rare de rhinocérotidés (Mammalia, Perissodactyla) dans le Miocène inférieur de Pellecahus (Gers, France). *Geobios* 33:249–255. DOI: 10.1016/S0016-6995(00)80022-4.

Antoine P-O, Downing KF, Crochet J-Y, Duranthon F, Flynn LJ, Marivaux L, Métais G, Rajpar AR, Roohi G. 2010. A revision of *Aceratherium blanfordi* Lydekker, 1884 (Mammalia:

509 Rhinocerotidae) from the Early Miocene of Pakistan: postcranials as a key: MIOCENE
510 RHINOCEROTIDS FROM PAKISTAN. *Zoological Journal of the Linnean Society*
511 160:139–194. DOI: 10.1111/j.1096-3642.2009.00597.x.
512 Antoine P-O, Métais G, Orliac MJ, Crochet J-Y, Flynn LJ, Marivaux L, Rajpar AR, Roohi G,
513 Welcomme J-L. 2013. Mammalian Neogene Biostratigraphy of the Sulaiman Province,
514 Pakistan. In: Fortelius M, Wang X, Flynn L eds. *Fossil Mammals of Asia*. Columbia
515 University Press, 400–422. DOI: 10.7312/columbia/9780231150125.003.0016.
516 Antunes M, Ginsburg L. 1983. Les rhinocerotides du Miocene de Lisbonne-systematique,
517 ecologie, paleobiogeographie, valeur stratigraphique. *Ciencias da Terra (UNL)* 7:17–98.
518 Becker D, Tissier J. 2020. Rhinocerotidae from the early middle Miocene locality Gračanica
519 (Bugojno Basin, Bosnia-Herzegovina). *Palaeobiodiversity and Palaeoenvironments*
520 100:395–412. DOI: 10.1007/s12549-018-0352-1.
521 Blanchon M, Antoine P-O, Blondel C, De Bonis L. 2018. Rhinocerotidae (Mammalia,
522 Perissodactyla) from the latest Oligocene Thézels locality, SW France, with a special
523 emphasis on Mesaceratherium gaimersheimense Heissig, 1969. *Annales de Paléontologie*
524 104:217–229. DOI: 10.1016/j.annpal.2018.06.001.
525 Borissiak A. 1915. Mammifères fossiles de Sebastopol, II. *Trudy Geologicheskogo Komiteta,*
526 *Novaja Seria* 137:1–47.
527 Cerdeño E, Sanchez B. 2000. Intraspecific variation and evolutionary trends of *Alicornops*
528 *simorrense* (Rhinocerotidae) in Spain. *Zoologica Scripta* 29:275–305. DOI:
529 10.1046/j.1463-6409.2000.00047.x.
530 Chen GF, Wu WY. 1976. Miocene mammalian fossils of Jiulongkou, Cixian district, Hebei. *Vert*
531 *PalAsiat* 14:6–15.

532 Colbert EH. 1935. Siwalik mammals in the American Museum of Natural History. *Transactions*
533 *of the American Philosophical Society* 26:1–401.
534 Deng T. 2004. A new species of the rhinoceros *Alicornops* from the Middle Miocene of the
535 Linxia Basin, Gansu, China. *Palaeontology* 47:1427–1439. DOI: 10.1111/j.0031-
536 0239.2004.00420.x.
537 Deng T. 2005. New cranial material of *Shansirhinus* (Rhinocerotidae, Perissodactyla) from the
538 Lower Pliocene of the Linxia Basin in Gansu, China. *Geobios* 38:301–313. DOI:
539 10.1016/j.geobios.2003.12.003.
540 Deng T, Wang S, Xie G, Li Q, Hou S, Sun B. 2012. A mammalian fossil from the Dingqing
541 Formation in the Lunpola Basin, northern Tibet, and its relevance to age and paleo-
542 altimetry. *Chinese Science Bulletin* 57:261–269. DOI: 10.1007/s11434-011-4773-8.
543 Deng T, Wang WM, Yue LP. 2003. Recent advances of the establishment of the Shanwang
544 Stage in the Chinese Neogene. *Vert PalAsiat* 41:314–323. DOI: 10.19615/j.cnki.1000-
545 3118.2003.04.006.
546 Goloboff PA, Farris JS, Nixon KC. 2008. TNT, a free program for phylogenetic analysis.
547 *Cladistics : the international journal of the Willi Hennig Society* 24:774–786. DOI:
548 10.1111/j.1096-0031.2008.00217.x.
549 Guérin C. 1980. Les rhinocéros (Mammalia, Perissodactyla) du Miocène terminal au Pléistocène
550 supérieur en Europe occidentale. Comparaison avec les espèces actuelles (fascicule 1).
551 *Travaux et Documents des Laboratoires de Géologie de Lyon* 79:1–1184.
552 Heissig K. 1969. *Die Rhinocerotidae (Mammalia) aus der oberoligozänen Spaltenfüllung von*
553 *Gaimersheim bei Ingolstadt in Bayern und ihre phylogenetische Stellung.* München :

554 Verlag der Bayerischen Akademie der Wissenschaften; in Kommission bei der C. H.
555 Beck'schen Verlagsbuchhandlung,.
556 Heissig K. 1972. Die obermiozäne Fossil-Lagerstätte Sandelzhausen. 5. Rhinocerotidae
557 (Mammalia), Systematik und Ökologie..pdf. In: *Die obermiozäne Fossil-Lagerstätte*
558 *Sandelzhausen 5. Rhinocerotidae (Mammalia), Systematik und Ökologie.* Mitteilungen
559 der Bayerischen Staatssammlung für Paläontologie und historische Geologie, 57–81.
560 Heissig K. 1999. Family Rhinocerotidae. In: *In: Rössner, G.E., Heissig, K. (Eds.), The Miocene*
561 *Land Mammals of Europe.* Verlag Dr. F. Pfeil, Munich, 175–188.
562 Heissig K. 2012. Les Rhinocerotidae (Perissodactyla) de Sansan. In: *S. Peigné and S. Sen (eds.),*
563 *Mammifères de Sansan*. Mémoires du Muséum National d'Histoire Naturelle de Paris,
564 317–485.
565 Lu X, Zheng X, Sullivan C, Tan J. 2016. A skull of *Plesiaceratherium gracile* (Rhinocerotidae,
566 Perissodactyla) from a new lower Miocene locality in Shandong Province, China, and the
567 phylogenetic position of *Plesiaceratherium*. *Journal of Vertebrate Paleontology*
568 36:e1095201. DOI: 10.1080/02724634.2016.1095201.
569 Mermier E. 1895. Sur la découverte d'une nouvelle espèce d'*Acerotherium* dans la Molasse
570 burdigalienne de Royans. *Annales de la Société Linnéenne de Lyon* 42:163–189.
571 Peter K. 2002. Odontologie der Nashornverwandten (Rhinocerotidae) aus dem Miozän (MN 5)
572 von Sandelzhausen (Bayern). *Zitteliana* 22:3–168.
573 Pilgrim GE. 1910. Notice on new mammal genera and species from the Tertiaries of India.
574 *Records of the Geological Survey of India* 15:63–71.

575 Répelin J. 1917. Études paléontologiques dans le Sud-Ouest de la France (Mammifères). Les
576 rhinocérotidés de l'Aquitanien supérieur de l'Agenais (Laugnac). *Annales du Musée*
577 *d'Histoire Naturelle de Marseille* 16:1–47.
578 Ringström T. 1924. Nashorner der hipparion-fauna nord-chinas. *Geological Survey of China,*
579 *Series C,* 11:1–156.
580 Sanisidro O. 2011. Descripción de algunos dientes de rhinocerotidae del Mioceno Inferior de
581 Estrepouy (Francia). *Estudios Geológicos* 67:419. DOI: 10.3989/egeol.40547.198.
582 Steininger FF. 1999. Chronostratigraphy, geochronology and biochronology of the Miocene
583 "European Land Mammal Mega-Zones" (ELMMZ) and the Miocene "Mammal-Zones
584 (MN-Zones)." In: *In: Rössner, G.E., Heissig, K. (Eds.), The Miocene Land Mammals of*
585 *Europe.* München, Verlag Dr. Friedrich Pfeil, 9–24.
586 Wang J. 2021. *Vegetation History in Northern China and its Response to Critical Geological*
587 *and Environmental Events since the Neogene*. Beijing: Institute of Vertebrate
588 Paleontology and Paleoanthropology, University of Chinese Academy of Sciences.
589 Wang W, Zhang P-Z, Kirby E, Wang L-H, Zhang G-L, Zheng D-W, Chai C-Z. 2011. A revised
590 chronology for Tertiary sedimentation in the Sikouzi basin: Implications for the tectonic
591 evolution of the northeastern corner of the Tibetan Plateau. *Tectonophysics* 505:100–114.
592 Wang S, Zong L, Yang Q, Sun B, LI Y, Shi Q, Yang X, Ye J, Wu W. 2016. Biostratigraphic
593 subdividing of the Neogene Dingjia'ergou mammalian fauna, Tongxin County, Ningxia
594 Province, and its background for the uplift of the Tibetan Plateau. *Quaternary Sciences*
595 36:789–809.
596 Yan DF. 1983. Über die klassifikation und morphologie des schädel von *Plesiaceratherium* .
597 *Vertebrata PalAsiatica* 21:134–143.

598 Yan D, Heissig K. 1986. Revision and autopodial morphology of the Chinese-European
599 rhinocerotid genus *Plesiaceratherium gracile* Young 1936. *Zitteliana, Munchen* 14:81–
600 109.
601 Young CC. 1937. On a Miocene mammalian fauna from Shantung. *Bulletin of the Geological*
602 *Society of China* 17:209–244.
603

# Figure 1

Photographs and sketches of the skull of *Plesiaceratherium tongxinense* sp. nov., holotype (IVPP V23959) a. dorsal view; b. lateral view; c. ventral view.

a. dorsal view; b. lateral view; c. ventral view.

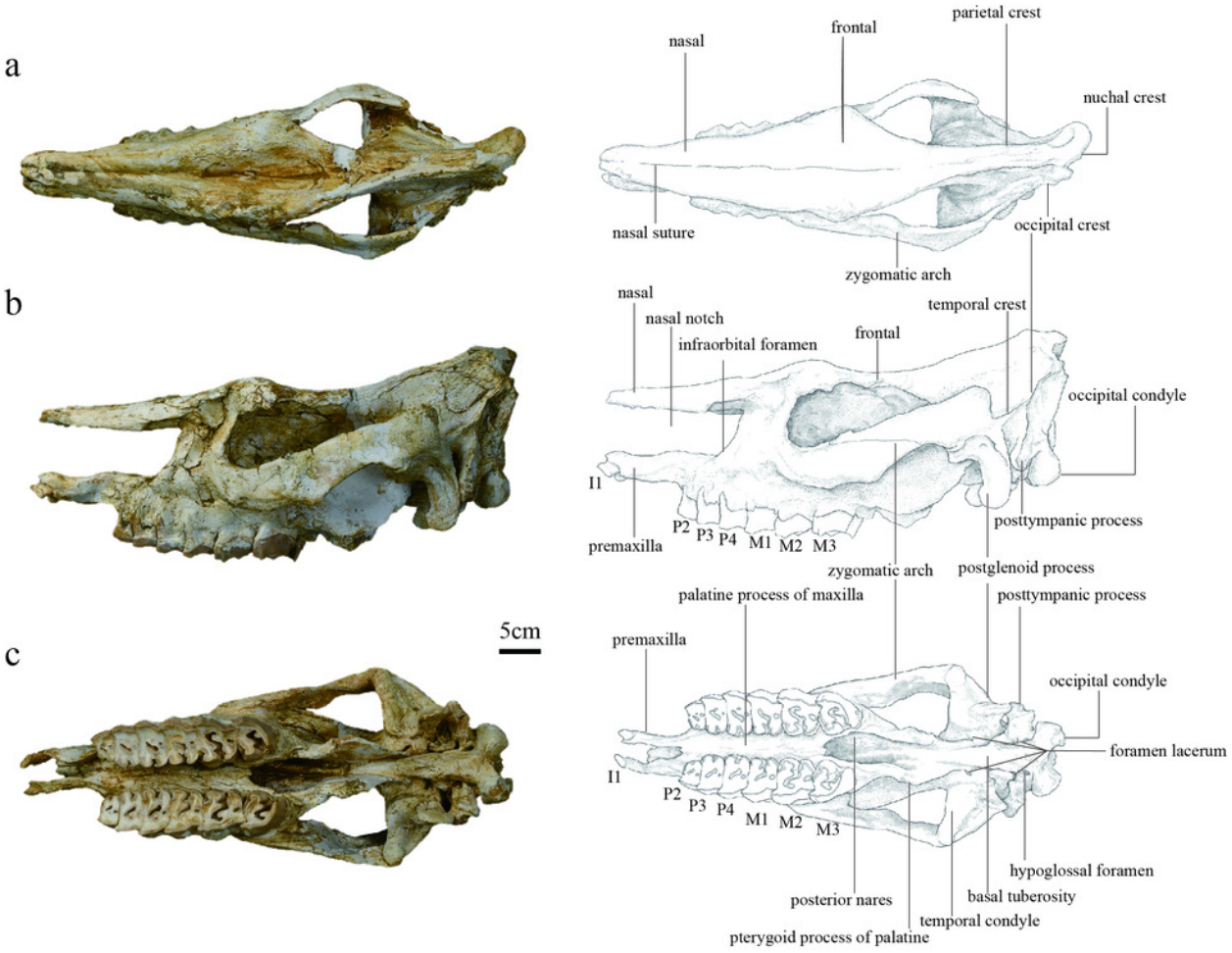

# Figure 2

Photograph of the posterior view of the skull of *Plesiaceratherium tongxinense* sp. nov., holotype (IVPP V23959).

# Figure 3

Photographs and sketches of the skull of *Plesiaceratherium tongxinense* sp. nov., holotype (IVPP V23959)

a. lateral view; b. occlusal view.

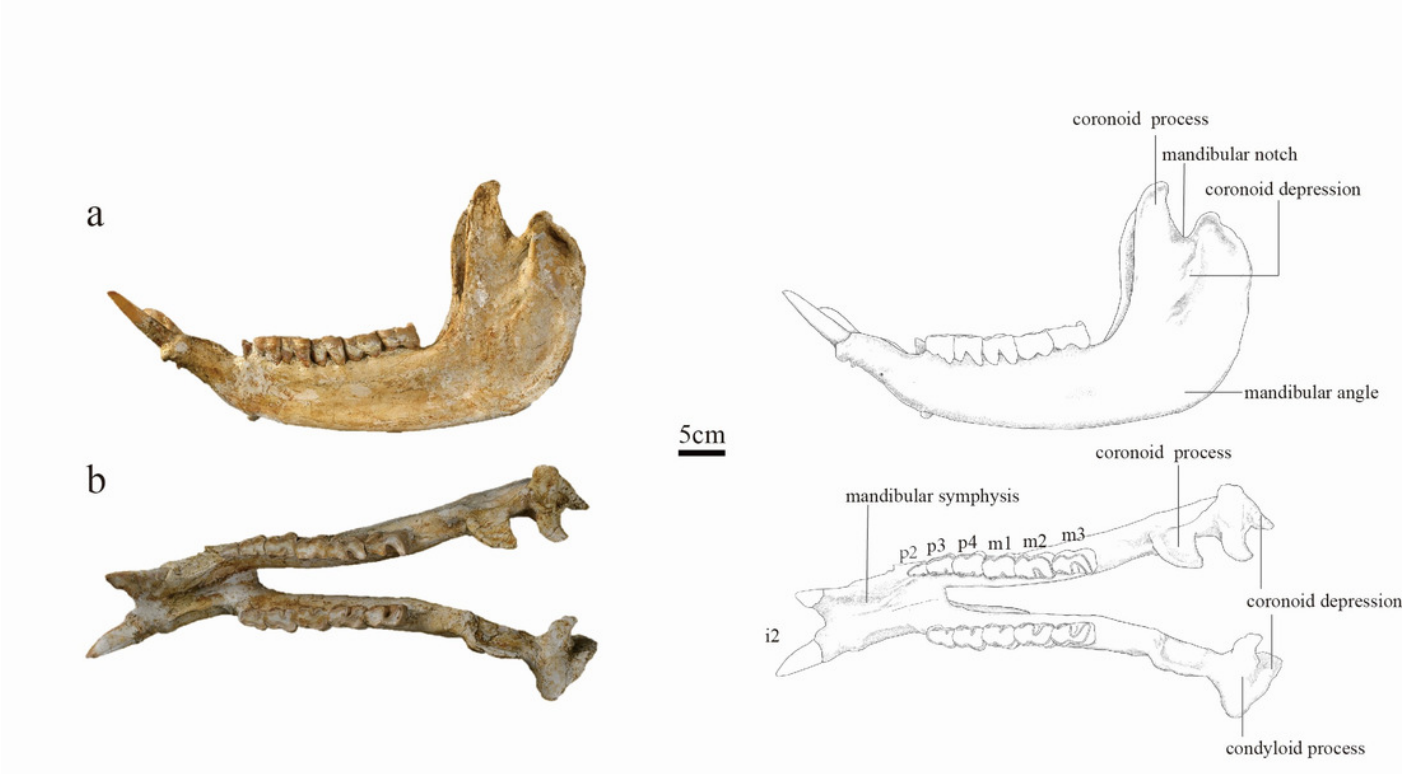

# Figure 4

Strict consensus of four most parsimonious trees showing phylogenetic positions of *Plesiaceratherium tongxinense* sp. nov.

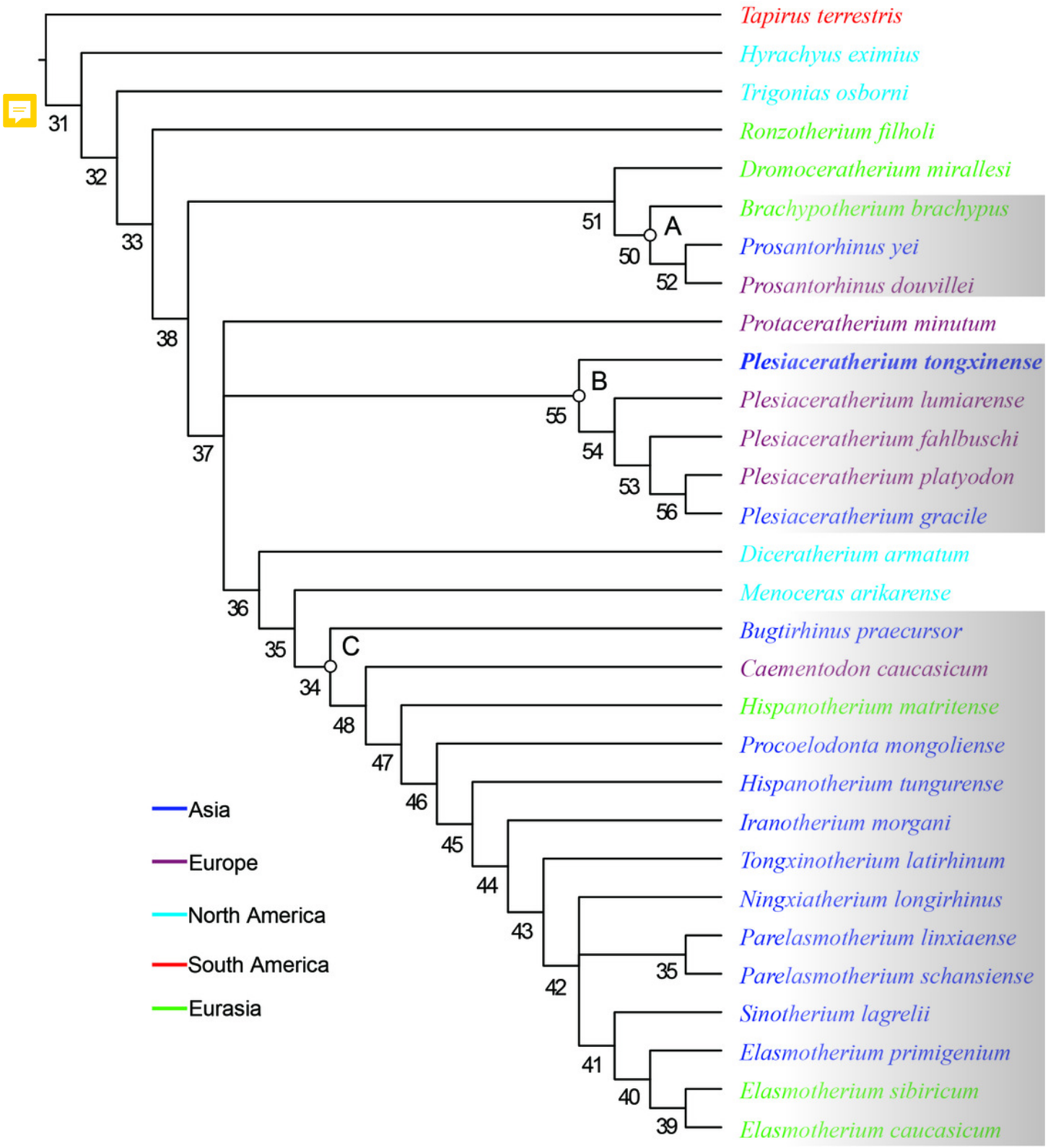
Tapirus terrestris
Hyrachyus eximius
Trigonias osborni
Ronzotherium filholi
Dromoceratherium mirallesi
Brachypotherium brachypus
Prosantorhinus yei
Prosantorhinus douvillei
Protaceratherium minutum
Plesiaceratherium tongxinense
Plesiaceratherium lumiarense
Plesiaceratherium fahlbuschi
Plesiaceratherium platyodon
Plesiaceratherium gracile
Diceratherium armatum
Menoceras arikarense
Bugtirhinus praecursor
Caementodon caucasicum
Hispanotherium matritense
Procoelodonta mongoliense
Hispanotherium tungurense
Iranotherium morgani
Tongxinotherium latirhinum
Ningxiatherium longirhinus
Parelasmotherium linxiaense
Parelasmotherium schansiense
Sinotherium lagrelii
Elasmotherium primigenium
Elasmotherium sibiricum
Elasmotherium caucasicum
A
B
C
31
32
33
51
50
52
38
37
55
54
53
56
36
35
34
48
47
46
45
44
43
42
35
41
40
39
Asia
Europe
North America
South America
Eurasia

## Table 1(on next page)

Measurements of the cheek teeth of *Plesiaceratherium tongxinense* sp. nov. and comparison with other *Plesiaceratherium* species. (mm)

**Table 1** Measurements of the cheek teeth of *Plesiaceratherium tongxinense* sp. nov. and comparison with other *Plesiaceratherium* species. (mm)(Measurements of *P. gracile*, *P. fahlbuschi*, *P. platyodon*, and *P. mirallesi* are from Yan and Heissig (1986); *P. lumiarense* is from Antunes and Ginsburg (1983) and Ginsburg and Bulot (1984))

| Teeth | | *P. tongxinense* sp. nov. | *P. gracile* | *P. fahlbuschi* | *P. platyodon* | *P. mirallesi* | *P. lumiarense* | *P. aquitanicum* | *P. balkanicum* |
|---|---|---|---|---|---|---|---|---|---|
| DP1 | L | - | - | - | 20 | 23 | 23 | - | 21 |
| | W | - | - | - | 18 | 20 | 19 | - | 20 |
| P2 | L | 28 | 31 | 24 | 30 | 29 | 29 | 29 | 29 |
| | W | 36 | 36 | 33 | 35 | 36 | 35 | 36 | 37 |
| P3 | L | 34 | 34 | 29 | 28 | 35 | 35 | 34 | 34 |
| | W | 45 | 42 | 39 | 43 | 45 | 44 | 46 | 43 |
| P4 | L | 39 | 37 | 32 | 34 | 38 | 38 | 36 | 35 |
| | W | 51 | 43 | 43 | 45 | 49 | 49 | 51 | 47 |
| M1 | L | 46 | 46 | 32 | 35 | 42 | 45 | - | 34 |
| | W | 53 | 48 | 44 | 43 | 47 | 49 | - | 41 |
| M2 | L | 54 | 48 | 36 | 38 | 46 | 45 | 47 | 38 |
| | W | 56 | 50 | 47 | 46 | 51 | 50 | 53 | 45 |
| M3 | L | 44 | 43 | 41 | 37 | 42 | 38 | 42 | 33-36 |
| | W | 52 | 45 | 42 | 42 | 45 | 49 | 49 | 37-40 |
| p2 | L | 23 | 28 | 26 | 27 | 32 | - | - | - |

| | | | | | | | | | |
|---|---|---|---|---|---|---|---|---|---|
| | W | 16 | 19 | 16 | 17 | 14 | - | - | - |
| p3 | L | 29 | 31 | 30 | 33 | 35 | - | - | - |
| | W | 23 | 20 | 19 | 23 | 21 | - | - | - |
| p4 | L | 37 | 35 | 32 | 33 | 39 | - | - | - |
| | W | 27 | 26 | 22 | 24 | 25 | - | - | - |
| m1 | L | 38 | 38 | 32 | 35 | 43 | - | - | - |
| | W | 28 | 28 | 22 | 24 | 23 | - | - | - |
| m2 | L | 44 | 40 | 37 | 38 | 46 | 42 | - | 36 |
| | W | 29 | 26 | 22 | 24 | 24 | 29 | - | 24 |
| m3 | L | 44 | 43 | - | 40 | 47 | 43 | - | 39 |
| | W | 27 | 27 | - | 23 | 25 | 27 | - | 24 |

**Table 2** Measurements of the skull of *Plesiaceratherium tongxinense* sp. nov. (IVPP V 23959). (mm) (Measurements of *P. gracile*, *P. fahlbuschi*, *P. platyodon*, and *P. mirallesi* are from Yan and Heissig (1986))

| numbers | measures | *P. tongxinense* sp. nov. | *P. gracile* | *P. fahlbuschi* | *P. platyodon* |
|---|---|---|---|---|---|
| 1 | Distance between occipital condyle and premaxilla | 584 | - | - | - |
| 2 | Distance between occipital condyle and nasal tip | 598 | 590-598 | 516 | 550 |

| | | | | | |
|---|---|---|---|---|---|
| 3 | Distance between nasal tip and occipital crest | 582 | - | - | - |
| 4 | Distance between nasal tip and bottom of nasal notch | 186 | 184-191 | 185 | 215 |
| 5 | Minimal width of braincase | 56 | - | - | - |
| 6 | Distance between occipital crest and postorbital process | 297 | - | - | - |
| 7 | Distance between occipital crest and supraorbital process | 329 | - | - | - |
| 8 | Distance between occipital crest and lacrimal tubercle | 376 | - | - | - |
| 9 | Distance between nasal notch and orbit | 67 | 66-67 | 43-35 | 58 |
| 13 | Distance between occipital condyle and M3 | 268 | | | |
| 14 | Distance between nasal tip and orbit | 243 | - | - | - |
| 15 | Width of occipital crest | 68 | - | - | - |
| 16 | Width of paramastoid process | 134 | - | - | - |
| 17 | Minimal width between parietal crests | 35 | - | - | - |
| 18 | Width between postorbital processes | 124 | - | - | - |
| 19 | Width between supraorbital processes | 139 | 182-186 | 175 | 178 |
| 20 | Width between lacrimal tubercles | 126 | - | - | - |
| 21 | Maximal width between zygomatic arches | 134 | 258-265 | 270 | 205 |
| 22 | Width of nasal base | 87 | 85-87 | 90-100 | 100 |
| 23 | Height of occipital surface | 149 | - | - | - |
| 25 | Cranial height in front of P2 | 145 | - | - | - |
| 26 | Cranial height in front of M1 | 176 | - | - | - |

| | | | | | |
|---|---|---|---|---|---|
| 27 | Cranial height in front of M3 | 189 | - | - | - |
| 28 | Width of palate in front of P2 | 40 | - | - | - |
| 29 | Width of palate in front of M1 | 35 | - | - | - |
| 30 | Width of palate in front of M3 | 41 | - | - | - |
| 31 | Width of foramen magnum | 38 | - | - | - |
| 32 | Width between exterior edges of occipital condyle | 97 | - | - | - |

8

| numbers | measures | *P. tongxinense* sp. nov. | *P. gracile* | *P. fahlbuschi* | *P. platyodon* |
|---|---|---|---|---|---|
| 1 | Distance between anterior end of symphysis and mandible angle | 470 | 433-435 | 435 | 455 |
| 2 | Distance between posterior end of symphysis and mandible angle | 317 | - | - | - |
| 3 | Height of horizontal part of ramus at posterior edge of p2 | 61 | - | - | - |
| 4 | Height of horizontal part of ramus at posterior edge of p3 | 65 | - | - | - |
| 5 | Height of horizontal part of ramus at posterior edge of p4 | 68 | - | - | - |
| 6 | Height of horizontal part of ramus at posterior edge of m1 | 80 | - | - | - |
| 7 | Height of horizontal part of ramus at posterior edge of m2 | 89 | - | - | - |
| 8 | Height of horizontal part of ramus at posterior edge of m3 | 98 | 79-88 | 85-77 | 85 |
| 9 | Transverse diameter of lingual edge of horizontal part of ramus at p4-m1 | 52 | - | - | - |
| 10 | Transverse diameter of lingual edge of horizontal part of ramus at anterior edge of m3 | 61 | 19-21 | 35 | 34 |

| | | | | | |
|---|---|---|---|---|---|
| 11 | Length of symphysis along median plane | 153 | 89-96 | 80-108 | 96 |
| 13 | Antero-posterior diameter of vertical part of ramus | 131 | - | - | - |
| 14 | Transverse diameter of condyle | 88 | - | - | - |
| 15 | Height of condyle | 238 | - | - | - |
| 16 | Height of coronoid process | 279 | - | - | - |

**Table 3** Measurements of the mandible of *Plesiaceratherium tongxinense* sp. nov. (IVPP V 23959). (mm) (Measurements of *P. gracile*, *P. fahlbuschi*, *P. platyodon*, and *P. mirallesi* are from Yan and Heissig (1986))